Decapentaplegic ligand ensures niche space restriction inside and outside of Drosophila testicular niche

Sharif M. Ridwan[1], Autumn Twille[1], Shinya Matsuda[2], Matthew Antel[1] and Mayu Inaba[1,*]

1. Department of Cell Biology, University of Connecticut Health Center, Farmington, Connecticut, United States of America
2. Biozentrum, University of Basel, Basel, Switzerland

[*] Correspondence: inaba@uchc.edu

Keywords: Germline stem cells, niche, Dpp, diffusion, Dedifferentiation, Morphotrap, Asymmetric division

Abstract

Drosophila male germline stem cells (GSCs) reside at the tip of the testis and surround a cluster of niche cells, called the hub. It has been believed that the Decapentaplegic (Dpp) ligand, secreted from the hub, only activates stem cells in close proximity, but not differentiating cells spaced one-cell layer away. However the range of Dpp diffusion is unknown. Here, using genetically encoded nanobodies, called Morphotrap, we physically block Dpp diffusion outside of the niche without interfering with niche-stem cell signaling. Surprisingly, we found that Dpp has an opposite effect on GSCs and on their immediate progenies, such that it promotes self-renewal of GSCs, while ensuring the differentiation of their daughter cells. When the signal from the diffusing fraction of Dpp was specifically blocked, differentiating daughter cells frequently dedifferentiated, suggesting that Dpp ensures asymmetric outcome of stem cells both inside and outside of the niche. We further show that these distinct signaling outcomes are achieved by the same canonical BMP pathway, through the typeI receptor, Thickveins (Tkv), and the downstream effector, Mothers against Dpp (Mad). Given the broad requirement of BMP pathway in many stem cell systems, we propose that such a self-contained behavior of a stem cell ligand may be a common mechanism to ensure special restriction of stem-cell niche.

Introduction

The stem cell niche was initially proposed to be a limited space in tissues or organs where tissue stem cells reside. Based on the phenomenon in which transplantation of hematopoietic stem cells is only successful when naïve stem cells are depleted, a niche is thought to provide a suitable environment for stem cells to self-renew[1,2]. At the same time, niche environment should not be preferable for differentiation of descendant cells so that correct balance of self-renewal and differentiation is maintained[2-4]. However, after more than 40 years since this niche concept was originally proposed[1], the mechanism of niche signal restriction is still largely unknown[5]. This is partly because of the difficulty of studying stem cells while located in *in vivo* tissues. Moreover, how broad signaling molecules secreted from the niche disperse is notoriously difficult to assess.

The *Drosophila* germline stem cell system provides a model to study niche-stem cell interaction. The niche, called the hub, is composed of post-mitotic hub cells. Each testis contains a single hub harboring 8-14 germline stem cells (GSCs) which directly attach to the hub[6]. The division of a GSC is almost always asymmetric via formation of stereotypically oriented spindle, producing a new GSC and a gonialblast (GB), the differentiating daughter cell[7]. After being displaced away from the hub, the GB enters 4 rounds of transit-amplifying divisions to form 2 to 16 cell spermatogonia (SGs). Then, 16-cell SGs become spermatocytes (SCs) and proceed to meiosis (Figure 1A-B)[8].

The Bone Morphogenetic Protein (BMP) ligand, Decapentapledic (Dpp) and Unpaird (Upd) have emerged as major niche ligands in the GSC niche[9-13]. In the testis, it has been hypothesized that these signals are only activated within GSCs in close contact to the hub, while immediately downregulated in GBs that are detached from the hub. However, the range of diffusion of these ligands have been unknown.

We previously demonstrated that hub-derived Dpp ligand is received by GSC-specific membrane protrusions, MT-nanotubes, to efficiently activate downstream pathways within the GSC population[14]. MT-nanotubes likely provide sufficient surface area along their length, allowing the plasma membranes of GSCs and hub cells to closely contact each other[14], suggesting the possibility that Dpp signal occurs in a contact-dependent manner.

In our previous study, we found that although Dpp ligand interacts with their receptor Dpp on the surface of MT-nanotubes[14], we also noticed that Dpp ligand from the hub can diffuse

farther away than previously thought[15], indicating that Dpp ligand secreted from the niche provide both contact-dependent and contact-independent signal. Besides the apparent contact-dependent signaling role of Dpp in the niche, we wondered if the diffusing fraction of Dpp ligand plays any role in the cells located outside of the niche.

In this study, we specifically address the function of the diffusing fraction of Dpp outside of the niche. We use a previously established tool, Morphotrap, which is a genetically encoded nanobody that can trap secretory ligands on the plasma membrane of ligand-secreting cells[16,17]. Unexpectedly, we found that Dpp has distinct roles on GSCs and differentiating germ cells, including promoting self-renewal of GSCs and blocking dedifferentiation of GBs and SGs.

Results

Dpp diffuses from niche to anterior area of testis

We previously showed that overexpressed Dpp ligand from the hub can diffuse outside of the niche[15]. However, we were not able to successfully visualize a diffusing fraction of Dpp when we used endogenously-tagged protein. For this study, we generated a fly line that exclusively expresses mGreen Lantern-tagged Dpp (*mGL-dpp*) at endogenous locus, as described previously[18], so that we can monitor endogenous Dpp behavior (Figure 1C). *mGL-dpp* lines were homozygous viable and no gross phenotypes were observed, indicating that the tagged Dpp protein is fully functional. Using these flies allowed us to successfully visualize endogenous Dpp expression and localization in the testis, as mGL-Dpp signal was seen throughout the tissue at levels above the background fluorescence (Figure 1D-E).

We noticed that mGL-Dpp localized in a pattern reminiscent of the extracellular space between cells throughout the testis, and not just at the niche (Figure 1E). Treatment of wild type testes with a diffusible 10KD dextran dye resulted in a similar pattern, as the dye could be seen throughout the tissue in extracellular spaces (Figure 1F). Both the dye and mGL-Dpp consistently appeared to surround interconnected germ cells at various stages of SG differentiation (Figure 1G-I), suggested a localization pattern around SG cysts, between the germline and the soma (Figure 1J).

As the localization pattern of the diffusible 10KD dextran dye and mGL-Dpp were similar, we hypothesized that the mGL-Dpp signal resulted from diffusion of the molecule from

the hub and throughout the tissue. To assess the capacity for mGL-Dpp to diffuse, we performed a fluorescence recovery after photobleaching (FRAP) analysis. After photobleaching, an average of ~20% of mGL-Dpp recovered (Figure 1K-K'), suggesting that there may be different fractions of the molecule present in the tissue: the mobile fraction which is freely diffusing likely from the niche, and an immobile fraction which is likely trapped in extracellular spaces or internalized by cells.

Taken together, these data indicate that a fraction of Dpp is mobile and likely diffuses throughout the extracellular space of the testis.

Perturbation of Dpp diffusion without affecting niche-GSC signal

While Dpp function is well-characterized in the niche, the role a potentially diffusible Dpp fraction outside of the niche is completely unknown. In order to assess the function of the diffusing fraction of Dpp, we sought to specifically disturb only the diffusing fraction of Dpp, without affecting niche-GSC signal. To achieve this, we utilized the morphotrap (MT), which is a genetically encoded tool consisting of a fusion protein between a transmembrane protein and a nanobody which acts as a synthetic receptor for tagged proteins[16,17]. We used two versions of MT each expressing a fusion protein between a nanobody recognizing Green fluorescent protein (GFP) or mGL, and two different transmembrane proteins (Figure 2A). Nrv-MT consists of the Nrv1 protein scaffold which has been known to localize basolateral compartment of the wing disc[17], where mCD8-MT consists of the membrane protein CD8 and tends to localize throughout the membrane[17]. In order to trap Dpp with MT, we utilized the hub driver fasIII-Gal4, which drives expression specifically in the hub cells (Figure 2B, C). By expressing MT under control of the fasIIIGal4 driver in the *mGL-dpp* homozygous background, we could effectively trap mGL-Dpp on cell membranes and thus prevent its diffusion (Figure 2B).

Indeed, expression of both Nrv-MT and mCD8-MT under fasIII-Gal4 driver eliminated mGL-Dpp signal throughout the testis (Figure 2D-F). fasIII>Nrv-MT showed mGL-Dpp signal enriched along the membrane, particularly at the hub-GSC interface (Figure 2G). In contrast, fasIII>mCD8-MT tended to show mGL-Dpp signal internalized within the hub (Figure 2H).

As fasIII>Nrv-MT results in mGL-Dpp trapped between the hub-GSC interface (Figure 2I), we hypothesized that hub-GSC Dpp signaling would remain intact in fasIII>Nrv-MT. To test this, we stained for pMad. fasIII>Nrv-MT showed similar pMad intensities in the GSCs to the

control sample (Figure 2M), indicating that Dpp signaling between the hub and the GSCs was preserved. pMad was reduced in GSCs of fasIII>mCD8-MT (Figure 2M), indicating defective signaling likely because of internalization and subsequent degradation (Figure 2I). It should be noted that in both conditions, trapping Dpp did not perturb pMad signal in somatic cyst cells (Figure S2A, B), which suggests that pMad in cyst cells is not activated by hub-derived diffusing Dpp and serves as a reliable internal control for quantifying relative pMad intensity in germ cells.

Importantly, expression of Nrv-MT using the germline driver nosGal4 resulted in mGL-Dpp trapping along the membranes of germ cells outside of the niche (Figure 2N, O) and activation of phosphorylated Mad (pMad), a readout for Dpp signaling, outside of the niche (Figure 2P, Q). These data further confirm that a fraction of Dpp is diffusible and trappable by the MT method, and trapped Dpp can still signal to the receptor present on the plasma membrane of the same cells.

Based on these results, fasIII>Nrv-MT expression in the *mGL-dpp* homozygous background can be used to assess the function(s) of hub-derived Dpp outside of the niche, without disrupting hub-GSC Dpp signaling.

Diffusing fraction of Dpp prevents dedifferentiation

In *Drosophila* testis, GSCs almost exclusively divide asymmetrically, resulting in one GSC and on GB (asymmetric outcome, Figure 3A); however, in some cases a GSC division can result in a symmetric outcome (Figure 3A). Symmetric events occur via two mechanisms: 1) spindle misorientation, where the mitotic spindle orients parallel to the hub-GSC interface, resulting in two GSCs (Figure 3A-□)[7], and 2) dedifferentiation, where a differentiated GB or SG "crawls back" to the niche and reverts to a GSC identity (Figure 3A-□)[19].

By scoring for the orientation of the cells still interconnected by fusome, a germline-specific organelle which branches throughout germ cells during division, we can estimate the frequency of symmetric events in the niche[19-21]. We noticed that fasIII>Nrv-MT testes showed a significantly higher frequency of symmetric events than the control (Figure 3B-D), suggesting that preventing Dpp diffusion results in more GSC symmetric outcomes.

Although fasIII>Nrv-MT expression results in increased symmetric events in GSC division, pMad levels in GSCs remain normal (Figure 2I-J), suggesting GSCs may not be directly affected in this genotype. Moreover, the number of GSCs at the hub were significantly

higher in fasIII>Nrv-MT testes at timepoints of day 14 and 21 post-eclosion (Figure 3E), suggesting that increased symmetric events are unlikely the consequence of GSC loss. We therefore considered the possibility that increased dedifferentiation rather than symmetric division might be responsible for observed high frequency of symmetric events. To test this hypothesis, we utilized a previously-described method of heat-shock (hs) inducible expression of *bag of marbles* (*bam*)[19], which is a translational repressor that is expressed after a germ cell exits the GSC state and is sufficient for promoting differentiation[19]. Using this system, we can artificially induce differentiation of GSCs by temporal heat shock, resulting in no GSCs remaining at the niche. After the flies are allowed to recover, the cells present at the niche represent germ cells which have dedifferentiated. By introducing *hs-bam* transgene in the *mGL-dpp* homozygous background with or without *fasIII>nrv-MT*, we can assess the potential role of the diffusible Dpp fraction on dedifferentiation. Strikingly, we observed that heat shock of Dpp trapped fly (*hs-bam, mGL-dpp, fasIII>nrv-MT),* barely resulted in a complete depletion of the GSC pool, and furthermore resulted in a significantly faster recovery of GSCs as compared to testes without MT (*hs-bam, mGL-dpp)*. While this data suggests that diffusible Dpp plays a role in dedifferentiation, it may also promote symmetric GSC division. To test this, we assessed the centrosome and spindle orientations of GSCs in the *dpp>nrv-MT* condition. While spindles were correctly oriented, indicating a lack of symmetric divisions, centrosomes of *dpp>nrv-MT* were significantly more misoriented (Figure 3I-M), likely as a result of a higher frequency of dedifferentiation as dedifferentiated GSCs are reported to have higher instances of centrosome misorientation[22].

Dpp acts through its canonical pathway both in GSC and in differentiating germ cells

We next asked if Dpp acts within the same signaling pathway in differentiating germ cells as it does in GSCs. Dpp is known to bind to its receptor Thickveins (Tkv) on GSCs and activate Tkv-mediated signaling to maintain GSC identity[9,10]. Knock-down of *tkv* by expression of shRNA under control of the germline driver *nosGal4* results in a depletion of GSCs from the niche (Figure 4A-B), demonstrating the indispensability of this pathway on GSC maintenance consistent with previous reports[9,10].

To determine if Tkv is the receptor for diffusible Dpp for germ cells outside of the niche, we knocked-down Tkv exclusively in differentiating germ cells using the driver bamGal4.

Intriguingly, we observed a higher number of GSCs per niche in *bam>tkvRNAi* testes as flies aged, similar to the observation of *mGL-Dpp, fasIII>nrv-MT* (Figure 3E). Moreover, *bam>tkvRNAi* testes also exhibit a higher frequency of symmetric events (Figure 4D-F), recapitulating the phenotype of *mGL-Dpp, fasIII>nrv-MT* and suggesting that Tkv-mediated signaling in differentiating germ cells may similarly result in higher instances of dedifferentiation. Indeed, analysis of flies expressing *hs-bam* and *bam>tkvRNAi* show a significantly faster recovery of GSCs after heat shock (Figure 4G), indicating Tkv-mediated signaling impedes dedifferentiation. Finally, we knocked-down Mad, the downstream effector of Tkv-signaling, and Medea, the partner of Mad, using bamGal4 mediated shRNA expression and found that both RNAi samples show a significantly faster recovery of GSCs after heat shock, indicating the Tkv-Mad/Medea pathway that is responsible for maintenance of GSCs, is also responsible for preventing dedifferentiation.

As was the case with Nrv-MT, centrosomes, but not spindles, were significantly more misorientated in all *bam>tkvRNAi*, *bam>madRNAi* and medeaRNAi (Figure 4H) suggesting that dedifferentiation, and not symmetric GSC division, is responsible for the increase in symmetric events.

Taken together, our data demonstrate a dual function of Dpp and its canonical signaling pathway in the *Drosophila* male germline. Contact-dependent Dpp signaling between the hub and GSCs promotes GSC maintenance, while contact-independent Dpp signaling arising from a hub-derived fraction of diffusible Dpp inhibits dedifferentiation of germ cells outside of the niche.

Discussion

In this study, we demonstrate that the diffusing fraction of a BMP ligand, Dpp, has function both on GSCs and on differentiating daughter cells. Surprisingly, Dpp has an opposite effect on these two populations, such that it promotes self-renewal of GSCs, while ensuring the differentiation of their daughter cells via preventing dedifferentiation. Furthermore, these distinct signaling outcomes are achieved by the same canonical BMP pathway, implying the importance of unknown intrinsic factor(s) on acquiring distinct signaling outcomes.

Signal from stem cell niche is believed to maintain “stemness” of resident stem cells. Therefore, the signal may not be preferable for differentiating daughter cells for initiating

differentiation program. In male and female germline stem cell system in Drosophila, a number of studies have revealed how a steep gradient of BMP response within a single cell diameter distance is established and thus contribute to asymmetric outcome of stem-cell division[23-34]. However, the Dpp ligand is also known as a major morphogen which diffuses over a long distance for patterning of embryo[35]. How can the same ligand create different level of gradient of cellular responses between these two systems? So far, no study has addressed whether Dpp ligand secreted from the niche has any function on differentiating descendants of stem cells.

Our study suggest a new model in which the BMP ligand can only simply diffuse away from the niche but can contribute to form steep gradient of signaling response which might be dictated by intrinsic difference of stem cell daughters. Since BMP ligands are broadly utilized ligand for many stem cell niches[36], we propose that this may be a common mechanism to ensure special restriction of stem-cell niche.

Acknowledgements

We thank Thomas Kornberg, Ryo Hattori and the Bloomington Drosophila Stock Center and the Developmental Studies Hybridoma Bank for reagents; Marie Bao (Life Science Editors) for manuscript editing. This research is supported by R35GM128678 from the National Institute for General Medical Sciences and start-up funds from UConn Health (to M.I.)

Author Contributions

M.I., S.M.R., A.T. and M.A. conceived the project, designed and executed experiments and analyzed data. S.A. designed and generated *mGL-dpp* line. M.A. and M.I., drafted manuscript. All authors edited the manuscript.

Declaration of Interests

The authors declare no competing interests.

Methods

Fly husbandry and strains

Flies were raised on standard Bloomington medium at 25°C (unless temperature control was required). The following fly stocks were obtained from Bloomington stock center (BDSC); *nosGal4* (BDSC64277); *hs-bam* (BDSC24636); *tkv RNAi* (BDSC40937); Nrv1 morphotrap (*lexAop-UAS-GrabFP.B.Ext.TagBFP*, BDSC68173); mCD8-morphotrap *(lexAop-UAS-morphotrap.ext.mCh*, BDSC68170); *medea RNAi:TRiP.GL01313* (BDSC43961); *mad RNAi:TRiP.JF01264* (BDSC31316); *dppGal4* (BDSC7007). *yw* (Stock #189, BDSC) was used for wildtype.

FasIII-Gal4 was obtained from DGRC, Kyoto Stock Center (A04-1-1 DGRC#103-948). *dpp-GFP* knock-in line was kind gift from Thomas Kornberg and Ryo Hattori. *UAS-histone H3-GFP* and *bam-Gal4* on 3rd was kind gifts from Yukiko Yamashita.

Generation of mGL-dpp allele

The detail procedure to generate endogenously tagged dpp alleles were previously reported[18]. In brief, utilizing the attP sites in a MiMIC transposon inserted in the dpp locus (MiMIC dppMI03752, BDSC36399), about 4.4 kb of the dpp genomic sequences containing the second (last) coding exon of dpp including a tag and its flanking sequences was inserted in the intron between dpp's two coding exons. The endogenous exon was then removed using FLP-FRT to keep only the tagged exon. mGL (mGreenLantern[37]) was inserted after the last processing site to tag all the Dpp mature ligands. *mGL-dpp* homozygous flies show no obvious phenotypes. The detail characterization of these alleles will be reported elsewhere.

Induction of dedifferentiation

Induction of dedifferentiation was performed following previously described method with modifications[19]. Approximately 0- to 3-day-old adult males carrying hs-Bam (BDSC24636) transgene were raised in 22°C and heat-shocked in a 37°C water bath for 30 min twice daily. Vials were placed in a 29°C incubator between heat-shock treatments. After 6-time treatments, vials were returned to 22°C for recovery.

Immunofluorescence Staining

Testes were dissected in phosphate-buffered saline (PBS) and fixed in 4% formaldehyde in PBS for 30–60 minutes. Next, testes were washed in PBST (PBS + 0.3% TritonX-100) for at least 30

minutes, followed by incubation with primary antibody in 3% bovine serum albumin (BSA) in PBST at 4°C overnight. Samples were washed for 60 minutes (three times for 20 minutes each) in PBST, incubated with secondary antibody in 3% BSA in PBST at room temperature for 2 hours and then washed for 60 minutes (three times for 20 minutes each) in PBST. Samples were then mounted using VECTASHIELD with 4',6-diamidino-2-phenylindole (DAPI) (Vector Lab). For pMad staining, testes were incubated with 5% BSA in PBST for 30min at room temperature prior to primary antibody incubation to reduce background.

The primary antibodies used were as follows: rat anti-Vasa (1:20; developed by A. Spradling and D. Williams, obtained from Developmental Studies Hybridoma Bank (DSHB); mouse-anti-FasIII (1:20, 7G10-DSHB); mouse anti-γ-Tubulin (GTU-88; 1:400; Sigma-Aldrich); Rabbit anti-pMad (1:300, Cell Signaling); Mouse anti-phospho-Histone H3 (Ser10) Antibody, clone 3H10 (Sigma-Aldrich). The secondary antibodies used were Goat Anti-Rabbit IgG H&L (Alexa Fluor 488, Abcam, ab175652), AlexaFluor-conjugated secondary antibodies (Abcam) were used at a dilution of 1:400.

Live imaging

Testes from newly eclosed flies were dissected into Schneider's Drosophila medium containing 10% fetal bovine serum and glutamine–penicillin–streptomycin. These testes were placed onto Gold Seal Rite-On Micro Slides' 2 etched rings with media, then covered with coverslips. Images were taken using a Zeiss LSM800 confocal microscope with a 63× oil immersion objective (NA = 1.4) within 30 minutes. Dextran dye permeabilization assay was performed as described previously [38]. Briefly, testes were incubated with 10KDa dextran conjugated to AlexaFluor-647 (Thermo Fisher Catalog number: D22914) at a final concentration of 0.2µg/µl in 1 mL media for 10min then immediately subjected for imaging. For FM4-64 staining (Thermo Fisher, Catalog number: T13320), testes were incubated with 5µg/mL in 1 mL media for 10 minutes at room temperature then briefly rinsed with 1 mL of media 3 times prior to imaging. For all live imaging experiments, imaging was performed within 15 minutes.

FRAP analysis

Fluorescence recovery after photo-bleaching (FRAP) of mGL-Dpp signal was undertaken using a Zeiss LSM800 confocal laser scanning microscope with 63X/1.4 NA oil objective. Zen

software was used for programming each experiment. Encircled areas of interest (randomly chosen 5μm-diameter circles from the area within less than 40 μm away from the testis tip) were photobleached using the 488 nm laser (laser power; 100%, iterations; 10). Fluorescence recovery was monitored every 10 seconds. Background signal taken in outside of the tissue in each time point were subtracted from the signal of bleached region. % recovery was calculated as follows; Let It be the intensity at each time point (t), Ipost be the intensity at post-bleaching and Ipre be the intensity at pre-bleaching. The governing equation of % recovery is: % recovery= (It – Ipost / Ipre - Ipost) x100.

Quantification of pMad intensities

Quantification of pMad intensity. Integrated intensity of pMad in nucleus was measured for anti-pMad staining and divided by the area and background levels measured outside of the tissue were subtracted. For GSC, to normalize the staining condition, the average intensities of pMad from four cyst cells (CCs) in the same testes were used as internal control and the ratios of intensities were calculated as each GSC per average intensities of CC. The means and s.d. were plotted to the graph for each genotype.

Mean intensity values (a.u.) of CCs were unchanged for each genotype (Figure S2A, B).

Scoring of centrosome and spindle orientation

Centrosome misorientation was indicated when neither of the two centrosomes were closely associated with the hub-GSC interface during interphase. Spindle misorientation was indicated when neither of the two spindle poles were closely associated with the hub-GSC interface during mitosis.

Statistical analysis and graphing

No statistical methods were used to predetermine sample size. The experiments were not randomized. The investigators were not blinded to allocation during experiments and outcome assessment. All experiments were independently repeated at least twice to confirm the results. Statistical analysis and graphing were performed using GraphPad Prism 9 software. Data are means and standard deviations.

Supplemental Data Individual numerical values displayed in all graphs are provided.

Figure legends

Figure 1. Dpp diffuses from niche to anterior area of testis

A) Anatomy of anterior area of Drosophila testis. Hub cells form a cluster and serve as the niche for germline stem cells (GSCs). Differentiating daughter cells or gonialblasts (GBs) undergo 4 rounds of incomplete division, called spermatogonia (SGs). Somatic cyst stem cells (CySCs) or cyst cells (CCs) are encapsulating developing germline. **B**) A schematic of asymmetric division (ACD) of GSCs. When the GSC divides, the mitotic spindle is always oriented perpendicularly towards hub-GSC interface (left panel). As the result, GSC and GB are stereotypically positioned, one close to the hub and the other away from the hub (right column). Signal from the hub only activate juxtaposed daughter cell so that the two daughter cells can acquire distinct cell fates. **C**) A design of mGreen Lantern (mGL)-dpp cassette replaced with endogenous *dpp* coding region. **D, E**) Representative confocal images comparing testis tips isolated from wildtype (*yw*) and *mGL-dpp* line using the same setting for imaging. **F**) A representative confocal image of testis tips after incubated with Alexa Fluor 647 conjugated dextran-dye. Wildtype (*yw*) flies were used. **G-I**) Magnified SG areas of the testis from wildtype (*yw*, **G**) *mGL-dpp* fly (**H**) and the testis incubated with Alexa Fluor 647 dextran-dye (**I**). (**J**) Anatomical interpretation of images shown in **H** and **I**. **, K, K'**) Recovery curves of mGL-Dpp FRAP experiments. % recovery values (see Methods for caluculation) from all 14-time experiments are shown in **K**. Values from each trial are shown in different colors. **K'** shows average values.

All scale bars represent 10 μm. Asterisks indicate approximate location of the hub. In all images and graphs, live tissues were used.

Figure 2. Perturbation of Dpp diffusion without affecting niche-GSC signal

A) Schematics of the design to trap Dpp on the surface of Dpp producing cells using Morphotrap (MT), the genetically encoded synthetic receptor for GFP-tagged proteins. The nanobody, vhhGFP4 (blue circle), that specifically binds to GFP, is fused to extracellular domain of either mouse CD8 transmembrane protein (mCD8-MT) or Nrv1 basolateral protein scaffold (Nrv-MT). **B**) Expected outcome of hub-driven expression of morphotrap in the background of *mGL-dpp*

homozygous testis. Diffusing fraction of Dpp (left panel) will be trapped on the hub cell surface and no diffusing Dpp will be observed (right panel). **C**) Representative images of Histone H3-GFP expressed under hub-specific drivers, fasIII-Gal4. **D-F**) Representative images of *mGL-dpp* testis tip without (**D**) or with fasIII-Gal4 driven Nrv-MT expression (**E**) or with fasIII-Gal4 driven mCD8-MT expression (**F**). Arrowheads in **D** show mGL-Dpp signal along the surface of SG cysts. Such signal was completely disappeared in Morphotrap expressing samples (**E** and **F**). **G, H**) Representative images of trapped mGL-Dpp in the hub. Plasma membranes of cells are visualized by FM4-64 dye (red). Magnified images of squared regions in upper panels are shown in lower panels. A broken line in lower panel of **G** indicates trapped mGL-Dpp signal along hub-GSC interface. Arrowheads in lower panel of **H** indicate mGL-Dpp forming puncta within cytoplasm of hub cells, likely representing the internalized mGL-Dpp. **I**) Graphical interpretation of localization of trapped Dpp. **J-L**) Representative images of pMad staining of GSCs after trapping Dpp using indicated Morphotrap lines. fasIII-Gal4 driver was used. White broken lines encircle GSCs. **M**) Quantification of pMad intensity in GSCs (relative to CCs) of fasIII-Gal4 driven Nrv-MT or mCD8-MT expressing testes in *mGL-dpp* homozygous background. P-values were calculated by Dunnett's multiple comparisons test and provided as ** $P < 0.001$ or ns; non-significant ($P \geq 0.05$). **N, O**) Representative images of live testis tip of *mGL-dpp* fly without (**N**) or with (**O**) expressing Nrv-MT under the germline specific driver, nosGal4. Trapped mGL-Dpp signal is seen on the surface of early germ cells in **O** (white arrowheads). **P, Q**) pMad staining shows emerging pMad positive germ cells outside of the niche in *mGL-dpp, nos>nrv-MT* testis (arrowheads in **Q**). pMad positive germ cells are normally only seen in GSCs and immediate descendants around the hub (arrowheads in **P**). White broken lines encircle GSCs.
All scale bars represent 10 μm. Asterisks indicate approximate location of the hub. Live tissues were used for **C-F, G-H, N, O** and fixed samples were used for **J-L, P, Q**.

Figure S2. pMad intensity in CCs was unchanged upon perturbation of Dpp diffusion from the hub

A) Representative images of pMad staining in CC (marked by broken lines and arrowheads) of indicated genotypes. **B**) Quantification of pMad intensity in CCs of indicated genotypes. P-values were calculated by Dunnett's multiple comparisons test and provided as ns; non-significant ($P \geq 0.05$).

All scale bars represent 10 μm. Asterisks indicate approximate location of the hub. Fixed samples were used for all images and graphs.

Figure 3. Diffusing fraction of Dpp prevents dedifferentiation

A) Asymmetric and symmetric outcomes of GSC division. Symmetric outcome is defined as the case in which two daughter cells of a GSC division are both placed near the hub, resulting in production of two GSCs. It occurs as the consequence of either "symmetric division" or "dedifferentiation" (see details in main text). **B, C**) Representative images of testis tip without (**B**) or with (**C**) trapping Dpp. Broken lines indicate asymmetric events in **B** and a symmetric event in **C**. **D**) Frequency of testes showing any symmetric events without or with trapping Dpp. The p-value was calculated by student-t-test *** $P < 0.0001$. **E**) Change in GSC number during aging without or with trapping Dpp. P-values were calculated by Šídák's multiple comparisons test and provided as ** $P < 0.001$ or ns; non-significant ($P \geq 0.05$). **F, G**) Representative images of testis tip after depletion of GSC by expressing Bam (post HS; after 6-time heat shock treatment) and after 3-day recovery in room temperature culture without (**F**) or with (**G**) trapping Dpp. Broken lines indicate the edges of front most germ cells. **H**) Change in GSC number during recovery from forced differentiation of GSCs without or with trapping Dpp. P-values were calculated by Šídák's multiple comparisons test and provided as ** $P < 0.001$, **** $P < 0.00001$ or ns; non-significant ($P \geq 0.05$). **I-L**) Representative images of centrosomes (**I, J**) and spindles (**K, L**) of GSCs without (**I, K**) or with (**J, L**) trapping Dpp. **M**) Percentages of misoriented centrosome and spindle in GSCs without or with trapping Dpp. P-values were calculated by Šídák's multiple comparisons test and provided as **** $P < 0.00001$ or ns; non-significant ($P \geq 0.05$).

For trapping Dpp in this figure, Nrv-MT was expressed under the control of fasIII-Gal4 in *mGL-dpp* homozygous background. m*GL-dpp* homozygous flies without nrv-MT were used for control. Fixed samples were used for all images and graphs.

All scale bars represent 10 μm. Asterisks indicate approximate location of the hub.

Figure S3. Utilization of a combination of alternative genotypes

A) Change in GSC number during recovery from forced differentiation of GSCs. For trapping Dpp, Nrv-MT was expressed under the control of dpp-Gal4 in *GFP-dpp* homozygous

background. *GFP-dpp* homozygous knock-in flies without Nrv-MT expression were used for the control. P-values were calculated by Šídák's multiple comparisons test and provided as **** P < 0.00001 or ns; non-significant (P≥0.05). Fixed samples were used for scoring.

Figure 4. Dpp acts through its canonical pathway both in GSC and in differentiating germ cells

A, B) Representative images of testis tip without (**A**) or with (**B**) shRNA expression against *tkv* (tkv RNAi) under the *nosGal4* driver. **C**) Change in GSC number during aging without or with tkv RNAi expression under the *bamGal4* driver. P-values were calculated by Šídák's multiple comparisons test and provided as *** P < 0.0001 **** P < 0.00001 or ns; non-significant (P≥0.05). **D, E**) Representative images of testis tip without (**D**) or with (**E**) tkv RNAi expression under the *bamGal4* driver. Broken lines indicate symmetric events. **F**) Frequency of testes showing any symmetric events without or with *bam>tkv RNAi*. The p-value was calculated by student-t-test ** P < 0.001. **G, H**) Change in GSC number during recovery from forced differentiation of GSCs without or with *bam>tkv RNAi* (**G**), *mad RNAi, Medea RNAi* (**H**). P-values were calculated by Šídák's multiple comparisons test and provided as *P < 0.01, **P < 0.001 or ns; non-significant (P≥0.05). **I**) Percentages of misoriented centrosome and spindle in GSCs in indicated genotypes. P-values were calculated by Šídák's multiple comparisons test and provided as **** P < 0.00001 or ns; non-significant (P≥0.05). **J**) Model. Dpp ligand has effect on GSCs contact dependent manner and on differentiating germ cells (GBs and SGs) through diffusion from the hub. Dpp is required for stem cell maintenance (Stemness), whereas its diffusing fraction promotes differentiation of daughter cells via preventing dedifferentiation. It explains self-containing role of stem-cell niche, not only supporting maintenance of stem cells, but also promoting proper differentiation after just one cell division.

All scale bars represent 10 μm. Asterisks indicate approximate location of the hub. Fixed samples were used for all images and graphs.

References

1 Schofield, R. The relationship between the spleen colony-forming cell and the haemopoietic stem cell. *Blood Cells* **4**, 7-25 (1978).

2 Scadden, D. T. Nice neighborhood: emerging concepts of the stem cell niche. *Cell* **157**, 41-50, doi:10.1016/j.cell.2014.02.013 (2014).

3 Rando, T. A. Stem cells, ageing and the quest for immortality. *Nature* **441**, 1080-1086, doi:10.1038/nature04958 (2006).

4 Morrison, S. J. & Kimble, J. Asymmetric and symmetric stem-cell divisions in development and cancer. *Nature* **441**, 1068-1074, doi:10.1038/nature04956 (2006).

5 Inaba, M., Yamashita, Y. M. & Buszczak, M. Keeping stem cells under control: New insights into the mechanisms that limit niche-stem cell signaling within the reproductive system. *Molecular Reproduction and Development* **83**, 675-683, doi:https://doi.org/10.1002/mrd.22682 (2016).

6 Dansereau, D. A. & Lasko, P. The development of germline stem cells in Drosophila. *Methods Mol Biol* **450**, 3-26, doi:10.1007/978-1-60327-214-8_1 (2008).

7 Yamashita, Y. M., Jones, D. L. & Fuller, M. T. Orientation of asymmetric stem cell division by the APC tumor suppressor and centrosome. *Science* **301**, 1547-1550, doi:10.1126/science.1087795 (2003).

8 de Cuevas, M. & Matunis, E. L. The stem cell niche: lessons from the Drosophila testis. *Development* **138**, 2861-2869, doi:10.1242/dev.056242 (2011).

9 Shivdasani, A. A. & Ingham, P. W. Regulation of Stem Cell Maintenance and Transit Amplifying Cell Proliferation by TGF-β Signaling in Drosophila Spermatogenesis. *Current Biology* **13**, 2065-2072, doi:https://doi.org/10.1016/j.cub.2003.10.063 (2003).

10 Kawase, E., Wong, M. D., Ding, B. C. & Xie, T. Gbb/Bmp signaling is essential for maintaining germline stem cells and for repressing bam transcription in the Drosophilatestis. *Development* **131**, 1365-1375, doi:10.1242/dev.01025 (2004).

11 Leatherman, J. L. & Dinardo, S. Germline self-renewal requires cyst stem cells and stat regulates niche adhesion in Drosophila testes. *Nat Cell Biol* **12**, 806-811, doi:10.1038/ncb2086 (2010).

12 Schulz, C. *et al.* A misexpression screen reveals effects of bag-of-marbles and TGF beta class signaling on the Drosophila male germ-line stem cell lineage. *Genetics* **167**, 707-723, doi:10.1534/genetics.103.023184 (2004).

13 Tulina, N. & Matunis, E. Control of stem cell self-renewal in Drosophila spermatogenesis by JAK-STAT signaling. *Science* **294**, 2546-2549, doi:10.1126/science.1066700 (2001).

14 Inaba, M., Buszczak, M. & Yamashita, Y. M. Nanotubes mediate niche-stem-cell signalling in the Drosophila testis. *Nature* **523**, 329-332, doi:10.1038/nature14602 (2015).

15 Ladyzhets, S. *et al.* Self-limiting stem-cell niche signaling through degradation of a stem-cell receptor. *PLOS Biology* **18**, e3001003, doi:10.1371/journal.pbio.3001003 (2020).

16 Harmansa, S., Hamaratoglu, F., Affolter, M. & Caussinus, E. Dpp spreading is required for medial but not for lateral wing disc growth. *Nature* **527**, 317-322, doi:10.1038/nature15712 (2015).

17 Harmansa, S., Alborelli, I., Bieli, D., Caussinus, E. & Affolter, M. A nanobody-based toolset to investigate the role of protein localization and dispersal in Drosophila. *eLife* **6**, e22549, doi:10.7554/eLife.22549 (2017).

18 Matsuda, S. *et al.* Asymmetric requirement of Dpp/BMP morphogen dispersal in the Drosophila wing disc. *Nat Commun* **12**, 6435, doi:10.1038/s41467-021-26726-6 (2021).

19 Sheng, X. R., Brawley, C. M. & Matunis, E. L. Dedifferentiating Spermatogonia Outcompete Somatic Stem Cells for Niche Occupancy in the Drosophila Testis. *Cell Stem Cell* **5**, 191-203, doi:https://doi.org/10.1016/j.stem.2009.05.024 (2009).

20 Brawley, C. & Matunis, E. Regeneration of Male Germline Stem Cells by Spermatogonial Dedifferentiation in Vivo. *Science* **304**, 1331-1334, doi:doi:10.1126/science.1097676 (2004).

21 Sheng, X. R. & Matunis, E. Live imaging of the Drosophila spermatogonial stem cell niche reveals novel mechanisms regulating germline stem cell output. *Development* **138**, 3367-3376, doi:10.1242/dev.065797 (2011).

22 Cheng, J. *et al.* Centrosome misorientation reduces stem cell division during ageing. *Nature* **456**, 599-604, doi:10.1038/nature07386 (2008).
23 Guo, Z. & Wang, Z. The glypican Dally is required in the niche for the maintenance of germline stem cells and short-range BMP signaling in the Drosophila ovary. *Development* **136**, 3627-3635, doi:10.1242/dev.036939 (2009).
24 Liu, M., Lim, T. M. & Cai, Y. The Drosophila female germline stem cell lineage acts to spatially restrict DPP function within the niche. *Sci Signal* **3**, ra57, doi:10.1126/scisignal.2000740 (2010).
25 Harris, R. E., Pargett, M., Sutcliffe, C., Umulis, D. & Ashe, H. L. Brat promotes stem cell differentiation via control of a bistable switch that restricts BMP signaling. *Dev Cell* **20**, 72-83, doi:10.1016/j.devcel.2010.11.019 (2011).
26 Van De Bor, V. *et al.* Companion Blood Cells Control Ovarian Stem Cell Niche Microenvironment and Homeostasis. *Cell Rep* **13**, 546-560, doi:10.1016/j.celrep.2015.09.008 (2015).
27 Wang, X., Harris, R. E., Bayston, L. J. & Ashe, H. L. Type IV collagens regulate BMP signalling in Drosophila. *Nature* **455**, 72-77, doi:10.1038/nature07214 (2008).
28 Xia, L. *et al.* The niche-dependent feedback loop generates a BMP activity gradient to determine the germline stem cell fate. *Curr Biol* **22**, 515-521, doi:10.1016/j.cub.2012.01.056 (2012).
29 Eliazer, S. *et al.* Lsd1 restricts the number of germline stem cells by regulating multiple targets in escort cells. *PLoS Genet* **10**, e1004200, doi:10.1371/journal.pgen.1004200 (2014).
30 Tseng, C. Y. *et al.* Smad-Independent BMP Signaling in Somatic Cells Limits the Size of the Germline Stem Cell Pool. *Stem Cell Reports* **11**, 811-827, doi:10.1016/j.stemcr.2018.07.008 (2018).
31 Jiang, X. *et al.* Otefin, a nuclear membrane protein, determines the fate of germline stem cells in Drosophila via interaction with Smad complexes. *Dev Cell* **14**, 494-506, doi:10.1016/j.devcel.2008.02.018 (2008).
32 Xia, L. *et al.* The Fused/Smurf complex controls the fate of Drosophila germline stem cells by generating a gradient BMP response. *Cell* **143**, 978-990, doi:10.1016/j.cell.2010.11.022 (2010).
33 Schulz, C., Wood, C. G., Jones, D. L., Tazuke, S. I. & Fuller, M. T. Signaling from germ cells mediated by the rhomboid homolog stet organizes encapsulation by somatic support cells. *Development* **129**, 4523-4534, doi:10.1242/dev.129.19.4523 (2002).
34 Sardi, J. *et al.* Mad dephosphorylation at the nuclear pore is essential for asymmetric stem cell division. *Proceedings of the National Academy of Sciences* **118**, e2006786118, doi:doi:10.1073/pnas.2006786118 (2021).
35 Nellen, D., Burke, R., Struhl, G. & Basler, K. Direct and Long-Range Action of a DPP Morphogen Gradient. *Cell* **85**, 357-368, doi:https://doi.org/10.1016/S0092-8674(00)81114-9 (1996).
36 Zhang, J. & Li, L. BMP signaling and stem cell regulation. *Developmental Biology* **284**, 1-11, doi:https://doi.org/10.1016/j.ydbio.2005.05.009 (2005).
37 Campbell, B. C. *et al.* mGreenLantern: a bright monomeric fluorescent protein with rapid expression and cell filling properties for neuronal imaging. *Proceedings of the National Academy of Sciences* **117**, 30710-30721, doi:doi:10.1073/pnas.2000942117 (2020).
38 Fairchild, M. J., Islam, F. & Tanentzapf, G. Identification of genetic networks that act in the somatic cells of the testis to mediate the developmental program of spermatogenesis. *PLOS Genetics* **13**, e1007026, doi:10.1371/journal.pgen.1007026 (2017).

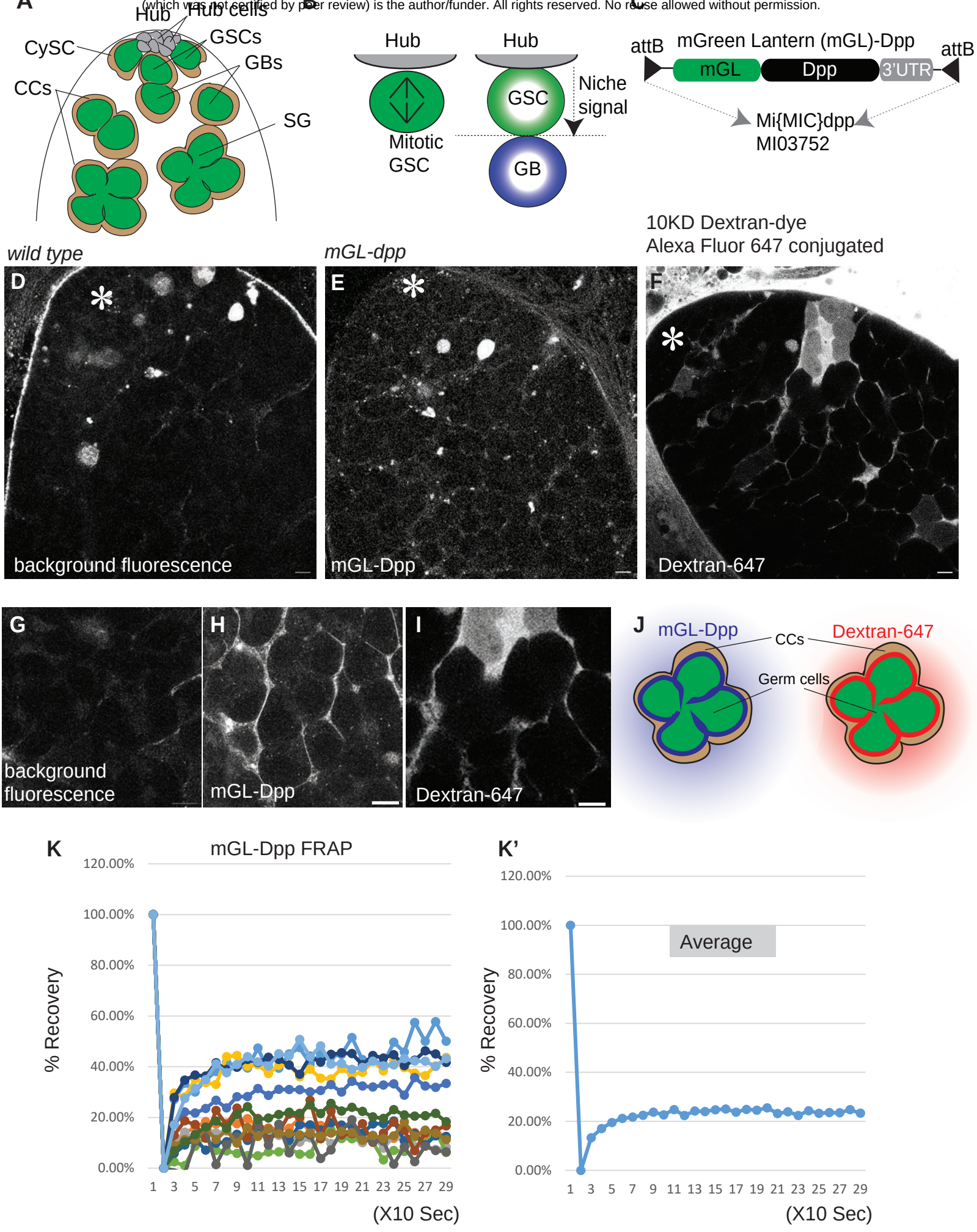

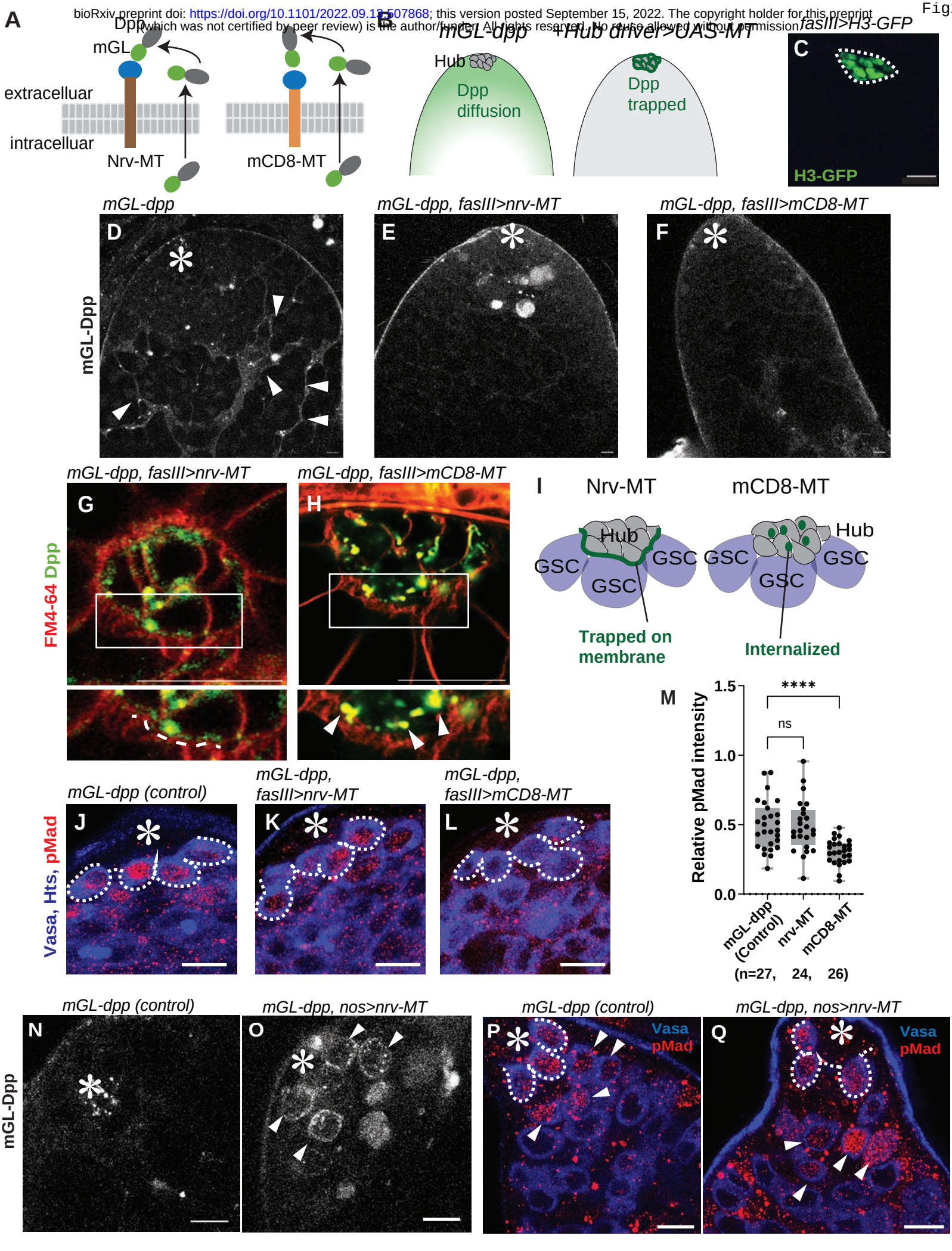

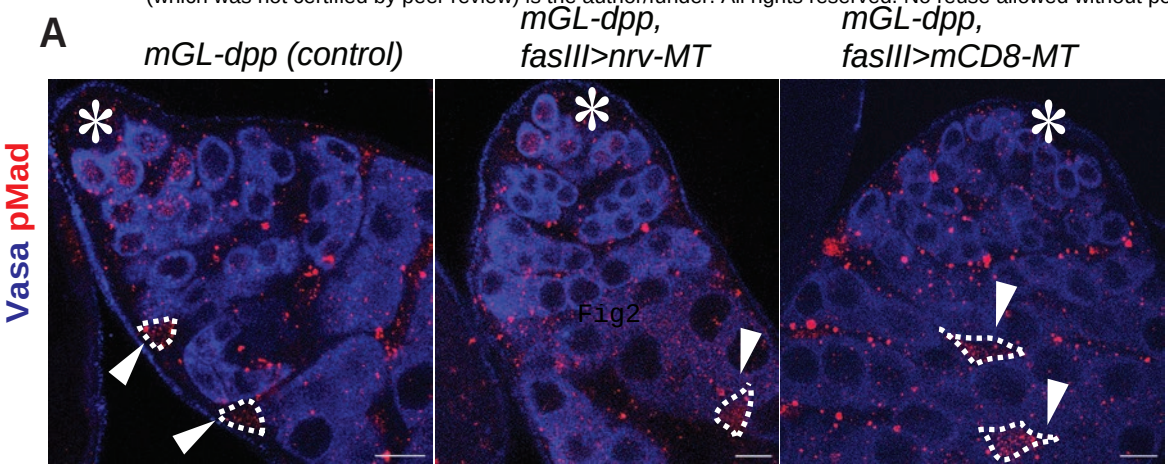

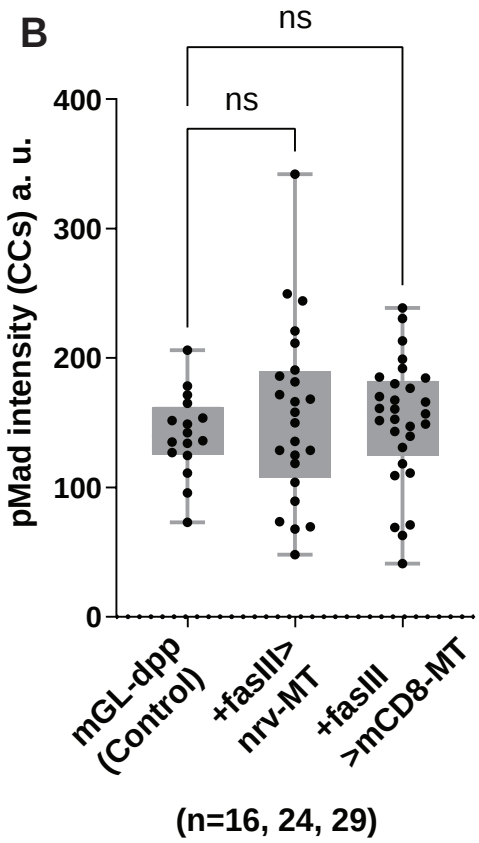

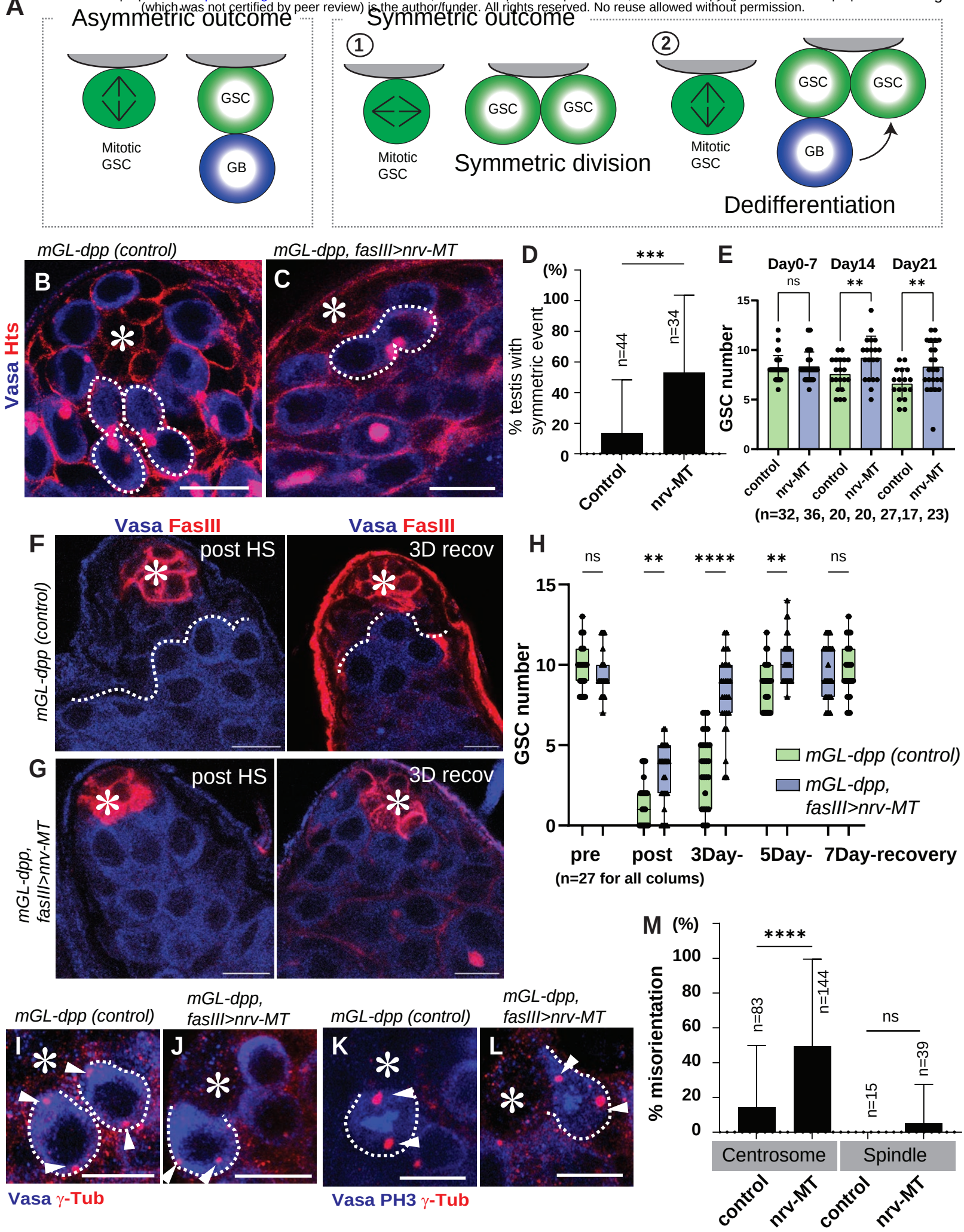

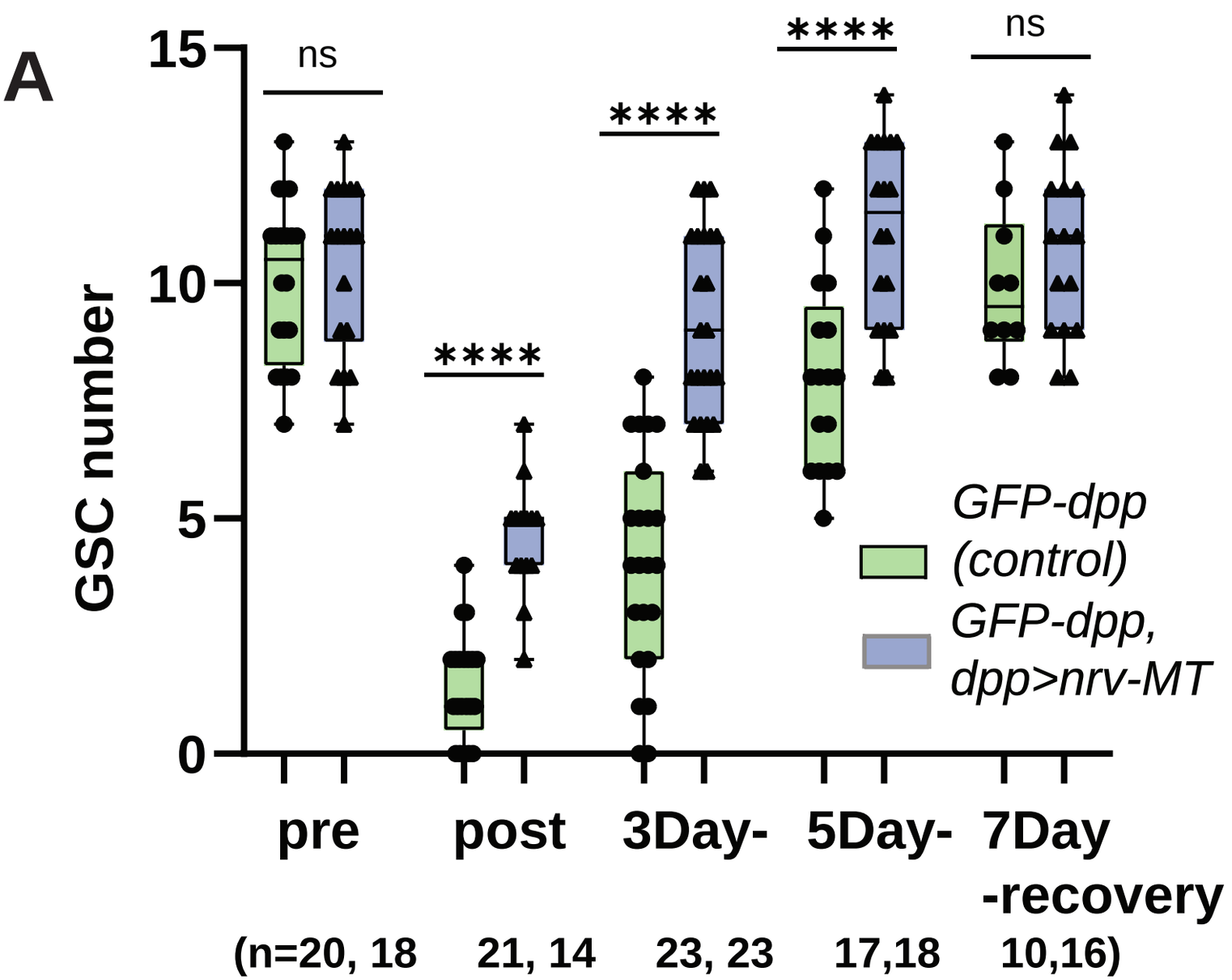
A
GSC number
15
10
5
0
ns
****
****
****
ns
GFP-dpp (control)
GFP-dpp, dpp>nrv-MT
pre
post
3Day-
5Day-
7Day -recovery
(n=20, 18
21, 14
23, 23
17,18
10,16)